

3D OPTICAL AND IR SPECTROSCOPY OF EXCEPTIONAL HII GALAXIES

E. Telles^{1,2}

RESUMEN

En esta contribución se presentará brevemente algunos resultados obtenidos al aplicar espectroscopía 3D a observaciones de la conocida galaxia HII II Zw 40, tanto en el óptico, como en el cercano infrarrojo. Se ha estudiado la distribución de polvo en la región del brote de formación, la velocidad y la dispersión de velocidades, y la geometría del hidrógeno molecular y el gas ionizado. Se encontró una clara correlación entre la componente del medio interestelar y el campo de velocidades, sugiriendo que la última tiene un rol fundamental en definir los modos del proceso de formación estelar.

ABSTRACT

In this contribution I will very briefly summarize some recent results obtained applying 3D spectroscopy to observations of the well known HII galaxy II Zw 40, both in the optical and near-IR. I have studied the distribution of the dust in the starburst region, the velocity and velocity dispersion, and the geometry of the molecular hydrogen and ionized gas. I found a clear correlation between the component of the ISM and the velocity field suggesting that the latter has a fundamental role in defining the modes of the star formation process.

Key Words: galaxies: evolution — galaxies: starburst — H II regions — ISM: general

1. THE INTERNAL KINEMATICS OF II ZW 40

Bordalo, Telles, & Plana (in preparation) conducted a study of the HII galaxy II Zw 40 with IFU at GEMINI. Our H α velocity and dispersion maps reveal complex structures associated with two dominant Super Star Clusters in the core region. High velocity regions are found in the low intensity line emission that poorly represent the kinematics observed in the integrated optical nebular lines.

An efficient method to diagnose kinematic features in GHII regions is using the *Intensity- σ* ($I-\sigma$) and *Intensity-Velocity* ($I-V$) diagrams (Muñoz-Tuñón et al. 1996; Yang et al. 1996). In Figure 1 we show the $I-\sigma$ plot for all field observed, excluding oversampled regions. The $I-\sigma$ plot for II Zw 40 shows exactly the same basic features found in previous works on GHII regions. The horizontal line in $I-\sigma$ plot shows the velocity dispersion of 33.5 km s⁻¹ derived from the integrated line profile. It is a characteristic value for II Zw 40 found in all intensity regions. The inclined bands identified by Muñoz-Tuñón et al. (1996) are also verified in the plot. High velocity dispersions reach peaks of 70 km s⁻¹ in low intensity regions.

Figure 1 also shows that the bright core component presents the same σ value as the integrated

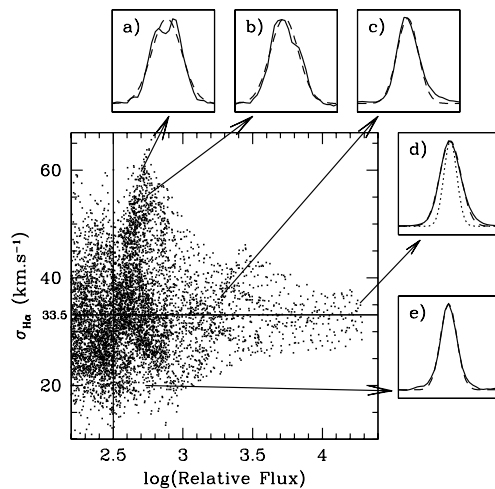


Fig. 1. $I-\sigma$ plots constructed for the total region observed in II Zw 40. The line profiles (a) and (b) are one of the most asymmetric and double peak profiles indicating expanding motions. The profile (c) is originated from the second brightest knot and shows a prominent red wing. The profile (d) comes from the brightest knot and (e) from the lowest dispersion region, both are very well represent by single gaussians.

profile and in fact dominates the overall dynamics of the system, being mostly responsible for the existing integrated luminosity and line width ($[L - \sigma]$) relation (see also Telles, Muñoz-Tuñón, & Tenorio-Tagle 2001).

¹On leave from Observatório Nacional, Rua José Cristino 77, Rio de Janeiro, 20921-400, Brazil (etelles@on.br).

²US Gemini Fellow, Astronomy Department, University of Virginia, Charlottesville, VA 22904, USA.

2. INTEGRAL FIELD NEAR INFRARED SPECTROSCOPY OF II ZW 40

Vanzi et al. (2008) have overcome the limits of the spatial resolution and the extinction effects in the optical by using Sinfoni/VLT with adaptive optics in the NIR on the prototypical HII galaxy II Zw 40. Spectroscopy in the near-IR gives access to different phases of the ISM: the ionized gas through the recombination lines of H and He, but also of other species as Iron; the warm molecular gas through the H_2 emission; and the dust through the ratios of well modeled lines as tracers of the extinction.

The emission of the forbidden lines of [FeII] occurs in partially ionized regions. Such regions can be found at the edge of HII regions, where however they are thin. Much more extended regions of partial ionization are produced by shocks. For this reason the [FeII] emission lines has proved to be an excellent tracer of SN remnants. The comparison with the contours of $Br\gamma$ shows that the centroids are almost coincident. We observe that the ratio FeII/ $Br\gamma$ is not uniform but has a value of about 0.06 compatible with pure photoionization and do not require the presence of supernovae, consistent with the extremely young age of the source.

We used images centered on $Br\gamma$ and Br11 to derive an extinction map of the galaxy. We observe from our extinction map how the extinction is not uniformly distributed. The asymmetry observed in the distribution of the dust is also observed often in galactic HII regions where young stars clean the ISM in preferential directions. In particular an extinction ridge is located between source A and source B. The average extinction over a region of 610 pix or about $10^5 pc^2$, is 3.78 mag. From this value, and using a ratio $N(HI)/A_v = 2 \times 10^{21} cm^{-2}/mag$ (Hunt et al. 2001) and we derive a dust mass of $2.8 \times 10^4 M_\odot$.

Several lines of H_2 are also detected in our spectra. The H_2 emitting region does not coincide with $Br\gamma$ and [FeII] and is significantly more extended and elongated in the NE direction. Contrary to what one would expect, there is no correlation between the H_2 emitting region and the spatial distribution of extinction. The detection of several H band lines and all 2-1S K band lines strongly suggests fluorescence as the excitation process. We do not detect any region where shocks significantly contribute to the excitation of H_2 . It is remarkable the detection of photon excited H_2 in region NE where basically no $Br\gamma$ emission is detected and the striking difference of geometry between H_2 , and $Br\gamma$, [FeII].

We derived radial velocity and velocity dispersion maps for the relevant lines by fitting gaussians to the

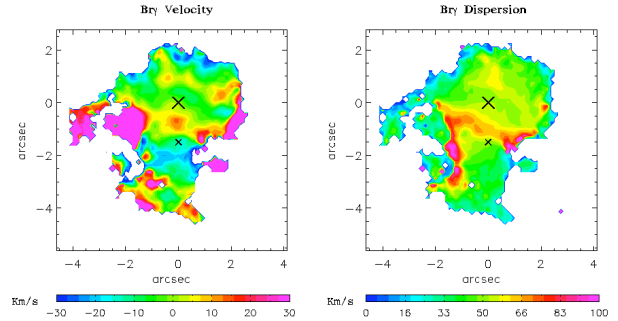


Fig. 2. $Br\gamma$ Velocity (left) and velocity dispersion (right) maps. Sources A and B are marked by crosses.

observed lines profiles (Figure 2). The nature and origin of the structure seen in the velocity map of $Br\gamma$ seems difficult to interpret. Their shape and orientation do not seem to be connected to the optical tails or the overall HI 21cm structure of the galaxy that are oriented toward south and southeast, nor do they show large velocity gradients. Thus, the dynamics of the star-bursting region is different and does not seem to have a clear connection with the large scale dynamics of the galaxy. The maps of [FeII] and H_2 cover a smaller region and are mostly flat. They show an intriguing difference in velocity among the lines: while the $Br\gamma$ average velocity is close to zero, [FeII] is redshifted by about $10-15 km s^{-1}$ and, most remarkably, H_2 is blueshifted by almost $90 km s^{-1}$. So not only is the H_2 cloud spatially distinct from the giant HII region at the center of II Zw 40, but it also has a very different velocity field.

We derived a velocity dispersion map for $Br\gamma$ only. These maps are in good agreement with the analogous kinematic analysis on $H\alpha$ maps by Bordalo, Telles, & Plana (in prep.). We also observe areas with high velocity dispersion coincident in some cases with regions of high radial velocity where the profiles typically show multiple components, indicative of wind-driven expanding bubbles. SNRs do not seem likely to play a relevant role in shaping the dynamics of the region.

REFERENCES

- Hunt, L. K., Vanzi, L., & Thuan, T. X. 2001, A&A, 377, 66
 Muñoz-Tuñón, C., Tenorio-Tagle, G., Castañeda, H. O., & Terlevich, R. 1996, AJ, 112, 1636
 Telles, E., Muñoz-Tuñón, C., & Tenorio-Tagle, G. 2001, ApJ, 548, 671
 Vanzi, L., Cresci, G., Telles, E., & Melnick, J. 2008, A&A, 486, 393
 Yang, H., Chu, Y.-H., Skillman, E. D., & Terlevich, R. 1996, AJ, 112, 146